Long Wavelength ($\lambda > 17$ μm) Distributed Feedback Quantum Cascade Lasers Operating in a Continuous Wave at Room Temperature

Hoang Nguyen Van, Zeineb Loghmari, Hadrien Philip, Michaël Bahriz, Alexei Baranov, Roland Teissier

photonics

MDPI

Article

Long Wavelength (λ > 17 μm) Distributed Feedback Quantum Cascade Lasers Operating in a Continuous Wave at Room Temperature

Hoang Nguyen Van †, Zeineb Loghmari, Hadrien Philip, Michael Bahriz, Alexei N. Baranov and Roland Teissier *

IES, University of Montpellier, CNRS, 34095 Montpellier, France;
nguyen.van.hoang@material.nagoya-u.ac.jp (H.N.V.); zeineb.loghmari@umontpellier.fr (Z.L.);
hadrien.philip@umontpellier.fr (H.P.); michael.bahriz@umontpellier.fr (M.B.);
alexei.baranov@umontpellier.fr (A.N.B.)
* Correspondence: roland.teissier@umontpellier.fr
† Present address: Graduate School of Engineering, Nagoya University, Chikusa-ku 464-8603, Nagoya, Japan.

Received: 1 March 2019; Accepted: 19 March 2019; Published: 21 March 2019

Abstract: The extension of the available spectral range covered by quantum cascade lasers (QCL) would allow one to address new molecular spectroscopy applications, in particular in the long wavelength domain of the mid-infrared. We report in this paper the realization of distributed feedback (DFB) QCLs, made of InAs and AlSb, that demonstrated a continuous wave (CW) and a single mode emission at a wavelength of 17.7 μm, with output powers in the mW range. This is the longest wavelength for DFB QCLs, and for any QCLs or semiconductor lasers in general, operating in a CW at room temperature.

Keywords: quantum cascade laser; distributed feedback; long wavelength infrared; molecular spectroscopy

1. Introduction

Quantum cascade lasers (QCLs) have become a very efficient and mature light source for the mid- to far-infrared [1]. Their wavelength coverage extends from 2.9 [2] to 20 μm [3] for room temperature operation and from 2.6 [4] to 200 μm [5] for cryogenic operation. The use of QCLs is particularly important for a wide range of gas sensing applications, owing to the fingerprints of many molecules in the MIR and FIR. The main spectral regions of interest for spectroscopy, which are explored today, lie in the MIR, in the bands close to 3.3, 5, 7.5, and 10 μm. Single frequency emission, required for molecular spectroscopy, can be obtained in distributed feedback (DFB) QCLs [6] that are a solution of choice for such applications targeting a specific absorption line. DFB QCLs operating in a continuous wave (CW) at room temperature have been demonstrated for wavelengths ranging from 4.3 [7,8] to 10.8 μm [9]

The extension of the available spectral range covered by QCLs would allow one to address new molecular species and new spectroscopy or gas sensing applications. The long wavelength domain above 10 μm is much less explored as compared to the 4–10 μm range since it is difficult to obtain high performance sources when the wavelength is increased. Yet, it is of interest for many applications such as the detection of C_2H_2 and aromatics such as benzene, toluene, and xylenes (BTEX) and the discrimination of common hydrocarbons such as propane. Other applications could be the use of long wavelength QCLs as local oscillators in heterodyne detectors for astronomy, e.g., for the detection of atomic oxygen around 17 μm. The manipulation of hyperfine states of donors in solids for

new quantum information technologies [10] and the spectroscopy of cold molecules for metrology experiments [11,12] are other applications that require suitable long wavelength laser sources.

The long wavelength range of the mid-infrared has been explored in the early years of QCLs, and cryogenic results were obtained, with wavelengths ranging from 17 [13] to as high as 24 µm [11]. Later, improved performances close to 15 µm were reported [14,15], and more recently the record was pushed to 28 µm [16]. Using the InP material family, the longest wavelength achieved by a QCL operating at room temperature is 16 µm [17]. DFB QCLs operating in pulsed mode were demonstrated at wavelengths of 13.8 [18] and 16 µm [17]. Using the alternative InAs/AlSb materials, CW operation at room temperature above a wavelength of 11 µm [19] and up to a wavelength of 15 µm [20] was demonstrated. With this technology, we achieved room temperature operation above 20 µm [3], and lasing was obtained up to 25 µm [21]. In this paper, we report significant progress with these lasers, with a record long wavelength operation of DFB QCLs in a continuous wave at room temperature at a wavelength of 17.7 µm.

2. Materials and Methods

The studied QCL is based on our previous developments of high gain InAs/AlSb active regions using a bound-to-bound vertical design [20]. The active quantum well (QW) and barrier thicknesses were adjusted in order to shift the emission wavelength to 17.5 µm (Figure 1). The dipole matrix element between the two active laser states *up* and *down*, spread over four coupled QWs, is z_{ud} = 6.2 nm. This large value, partly due to the low effective mass of conduction band electrons in InAs QWs, resulted in an oscillator strength of 73. Hence, even a low population inversion due to the short upper state lifetime (estimated to be 0.22 ps at room temperature) provides a large intersubband gain. We calculated a differential gain of the order of 40 cm/kA at room temperature, consistent with previous experimental data [3]. The injector is designed with a potential drop of about 100 meV under operating bias in order to limit the thermal population of the lower laser state and preserve population inversion at high temperature. This value, larger than the photon energy of 71 meV, introduces at significant voltage defect, but the voltage drop per period remains lower than 200 mV.

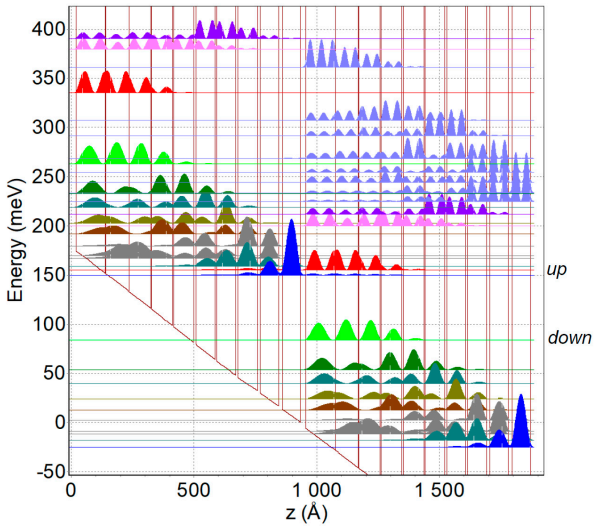

Figure 1. Band diagram of a portion of the studied active region. The laser transition is between the red (*up*) and green (*down*) states. Two quantum wells in the middle of the injector are doped with Si for an electron sheet density of 0.3 × 10^{11} cm^{-2} per stage.

The QCL structure was grown via solid source molecular beam epitaxy on an n-doped InAs substrate. It consisted of a lower cladding layer made of n-doped InAs, an undoped InAs waveguide layer, 55 stages of the active region pattern presented in Figure 1, an undoped InAs waveguide layer, and an n-doped InAs top cladding. The waveguide layers are 3 µm thick with a residual doping

$<10^{16}$ cm^{-2}. The cladding layers are 3 µm thick and doped with Si to a value of 4×10^{17} cm^{-3}. Due to free carriers, this doping level resulted in a reduction of the real part of the refractive index of about 0.45 relative to the waveguide layers for the design wavelength. The imaginary part of the refractive index in the cladding layers is calculated to be $k = 0.0098$. With these values, the fundamental TM guided mode in the QCL core region has calculated propagation losses of $\alpha_w = 5$ cm^{-1} and an overlap with the active region of $\Gamma = 64\%$.

Fabry–Pérot (FP) lasers were fabricated from this wafer, using the process described in [20], and characterized in pulsed mode at room temperature. The light intensity was measured with a pyroelectric detector whose response was first calibrated through the measurement of the average power on a power meter. The typical result is presented in Figure 2 for a 3.6-mm-long and 16-µm-wide QCL. The threshold current density was 1.0 kA/cm^2 at T = 25 °C, and the emission spectrum corresponding to the peak gain of the active zone was centered at a wavelength of 17.8 µm, close to the design target value. The typical spectral width of the gain in a QCL is of the order of 10% of the central wavelength. This allows the use of the same active region for the fabrication of DFB lasers with a relatively large detuning from the peak gain.

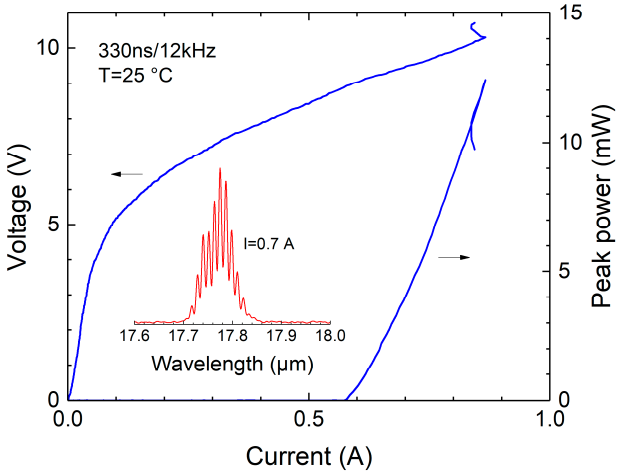

Figure 2. Room temperature electrical and optical characteristics of a typical FP quantum cascade laser (QCL) fabricated from the studied wafer. The laser is 3.6 mm long and 16 µm wide and driven with 330 ns current pulses at a repetition rate of 12 kHz. Inset: the pulsed emission spectrum of the laser.

The fabrication of high performance DFB QCLs usually relies on the implementation of a buried grating close to the active region [22]. This results in a pure index coupling that does not introduce additional propagation losses but that has a counterpart consisting in a competition between the two DFB modes located on the edges of the grating stop band. More complex designs are needed to avoid mode hopping, such as the use of a defect mode [23], a multi-section geometry [24], or an engineering of the facet reflectivity [25]. In addition, the regrowth of the top cladding on the buried grating is a complicated and expensive technological process. An alternative solution is the use of a grating on the top cladding layer made by a combination of etching and metal deposition [6]. This results in a complex coupling coefficient and possibly increased losses. The main advantage of this type of DFB is the efficient mode selection through the dissymmetry of the losses for the two band edge DFB modes as well as the simpler fabrication technology. Furthermore, it has been demonstrated that low loss, mostly index-coupled, modes could be selected through a proper choice of the grating depth [26]. In our case, we choose this solution with a grating etched into the top InAs cladding layer, then covered by the top metal contact layer. Prior to the grating fabrication, we thinned the cladding down to a thickness of 2.8 µm with inductively coupled plasma (ICP) dry etching in order to adjust the coupling strength for the chosen grating depth of 1.1 µm. Finite element electromagnetic modeling of this

patterned waveguide yielded a coupling coefficient of $\kappa = 12$ cm^{-1}, mostly real, and a loss contrast of 0.8 cm^{-1} between the two DFB modes.

The grating was defined by e-beam lithography. From the modeling and previous experimental data on similar waveguides, the effective index of the relevant mode was estimated to be $n_{eff} \approx 3.32$. Three different grating periods ($\Lambda = 2.666$, 2.600, and 2.590 µm) were defined on the same sample. The first one targeted the wavelength of the peak gain of the QCL's active zone, and the two smaller values targeted the wavelength of 17.2 µm (581 cm^{-1}) required for an application to the spectroscopy of cold CaF molecules. The grating was transferred to the InAs top cladding by ICP dry etching to a depth of 1.1 µm. The following fabrication steps were identical to those of FP lasers: UV contact lithography and wet etching to define 14-µm-wide and 11-µm-deep laser ridges, passivation using a polymerized resist, and top metal contact deposition. The devices were cleaved to form uncoated ≈ 3-mm-long cavities and mounted epi-side down on AlN submounts with indium.

3. Results and Discussion

The DFB lasers exhibited single frequency operation all over the tested temperature range, from 240 to 350 K, in pulsed mode. The emission peak at room temperature is plotted in Figure 3 as a function of the grating period for a set of QCLs. From these data, we extracted an effective index of 3.317±0.003. The $\Lambda = 2.666$-µm-lasers emitted at a wavelength near the peak gain of the active region. Their threshold current densities ($J_{th} = 1.02$ kA/cm^2) were very close to that of the FP lasers (Figure 4), which indicates that the DFB mode had propagation losses comparable to the FP modes. This is a confirmation that a top surface metallic grating with a well-designed geometry can be very efficient since the introduced additional loss is not significant. The lasers with a shorter grating period have their emission wavelength shifted by about 3% from the peak gain value. For these QCLs, J_{th} is 10% higher as compared to the FP lasers, due to the lower gain at the selected wavelength.

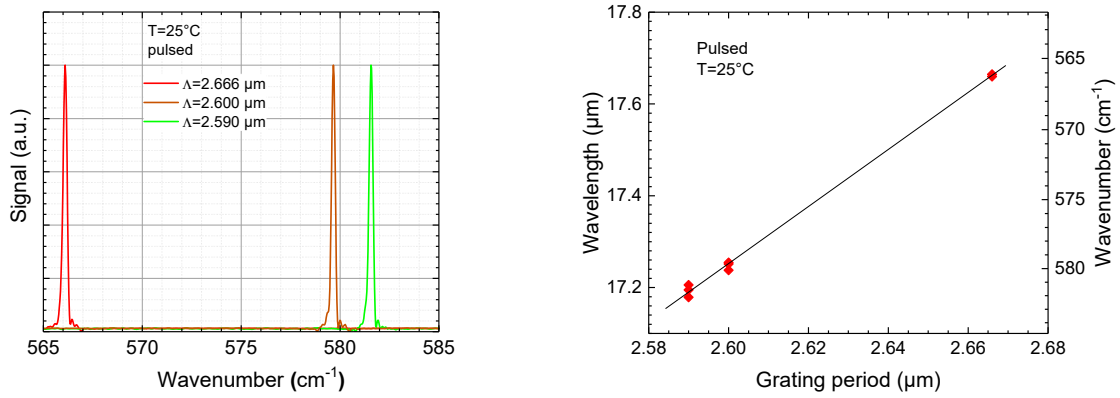

Figure 3. (**a**) Emission spectra in pulsed mode at 25 °C of DFB lasers with a different period of the DFB grating (Λ). The linewidth is limited by the resolution of the FTIR spectrometer. (**b**) Peak wavelength of the tested devices as a function of the period of the DFB grating.

The peak power measurements in different FP QCLs were similar. The corresponding average single-ended slope efficiency was 40 mW/A, without any correction. We estimated that the real value is about twice as large if we account for the optical setup transmission and collection efficiency. For the DFB QCLS, the slope efficiency varied substantially in different lasers. This is well-known to originate from the random phase of the cleaved output facet relative to the grating. The data presented in Figure 4 were obtained for selected DFB QCLs having the highest output power. There were still clear trends showing that DFB QCLs have lower power than FP QCLs, due to the relatively strong coupling ($\kappa L \approx 4$), and that DFB QCLs with a large detuning from the peak gain also have lower output power.

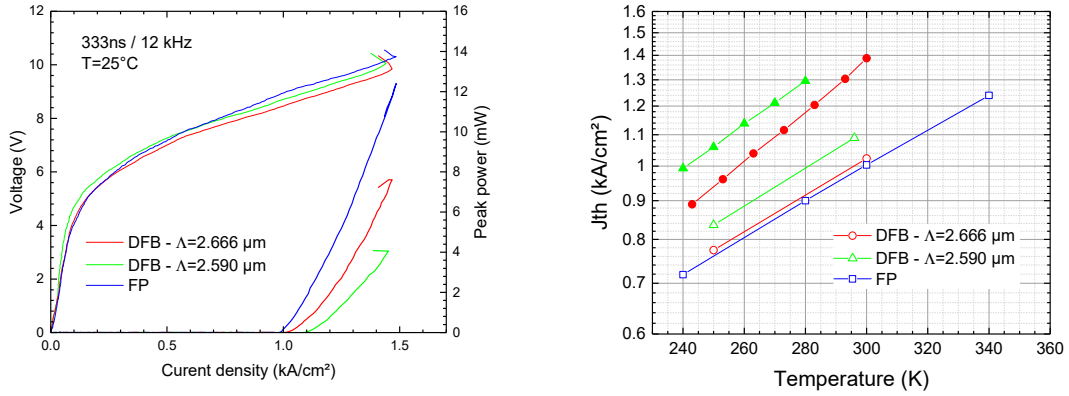

(**a**) (**b**)

Figure 4. (**a**) Comparison of the pulsed characteristics of FP and DFB QCLs with different grating periods. The FP laser is 3.6 mm long and 16 µm wide; the DFB laser with Λ = 2.666 µm is 3.4 mm long and 15 µm wide; the laser with Λ = 2.590 µm is 3.0 mm long and 14 µm wide. (**b**) Threshold current densities of the studied devices as a function of operating temperature. The open symbols are for pulsed operation, and the solid symbols are for CW operation.

The DFB lasers were tested in a continuous wave. The QCL with Λ = 2.666 µm operated in a CW up to a temperature of 300 K, with an uncorrected measured power of 6 mW at −30 °C and 0.5 mW at +20 °C (Figure 5). The emission was single mode, with no evidence of mode hopping, for the tested temperature range from −30 °C to +27 °C. The tuning range associated with this temperature interval was 3 cm^{-1}, corresponding to a relative change of 0.5%. This result sets the new record for the longest wavelength of 17.7 µm for single frequency DFB QCLs operating in a CW at room temperature. As a comparison, previously reported pulsed DFB QCLs have operated at 13.8 [18], 16 [17], and 17.8 µm [27] with a much higher J_{th}, whereas in the CW regime the longest reported wavelength was 10.8 µm [9].

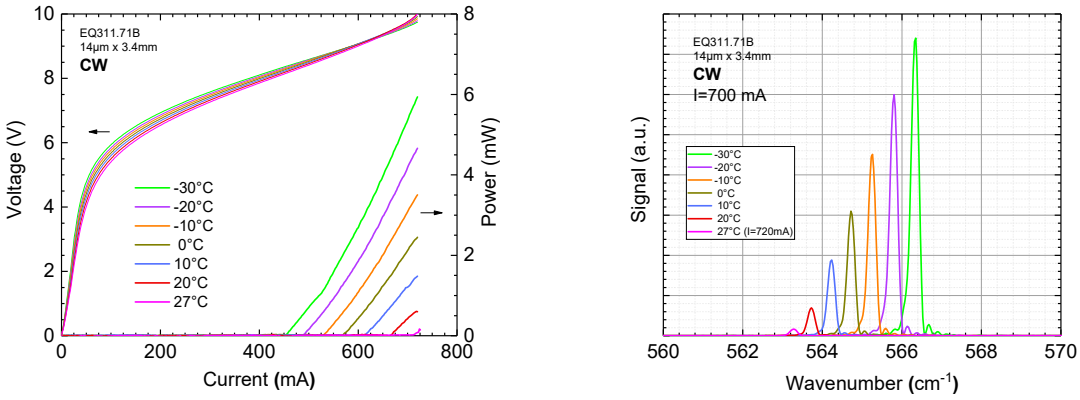

(**a**) (**b**)

Figure 5. (**a**) CW characteristics of a 3.4-mm-long and 14-µm-wide DFB QCL with Λ = 2.666 µm. The optical power is the power collected from one facet with a f/1 off-axis parabolic mirror without any correction for the collection efficiency. (**b**) Emission spectra in a CW as a function of the sample holder temperature for a current of 700 mA. The linewidth is limited by the resolution of the FTIR spectrometer.

The DFB QCLS with a detuning of 3% (Λ = 2.590 µm) also operated in a CW and in single mode, up to a temperature of 280 K (Figure 6). These lasers corresponded to the targeted wavenumber for the spectroscopy experiment on CaF cold molecules. The required spectral range around 581 cm^{-1} was accessible using one of these devices, integrated into a Peltier cooled module, with an available CW power greater than 1 mW. The measured temperature and current tuning rates were 0.054 cm^{-1}/K and 6.8 cm^{-1}/A, respectively.

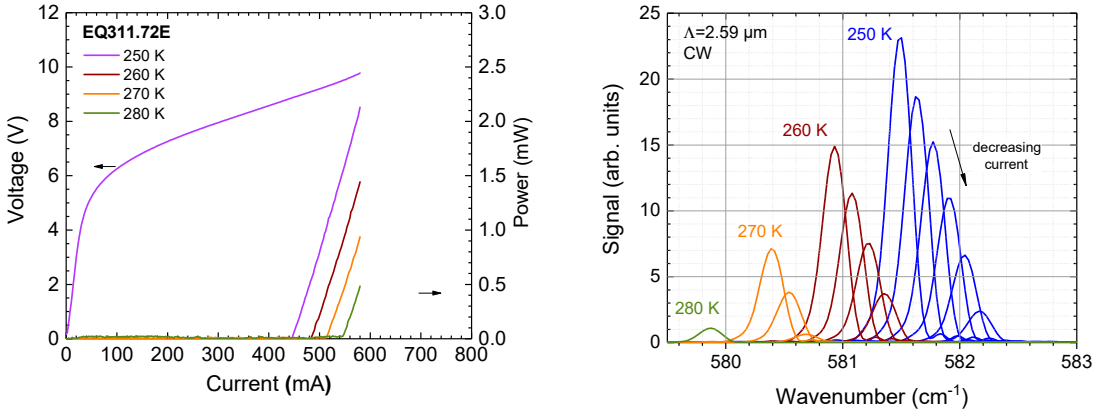

Figure 6. (**a**) CW characteristics of a 3.0-mm-long and 14-µm-wide DFB QCL with Λ = 2.590 µm, mounted in a Peltier cooled module. The optical power is the power collected from one facet with a f/1 off-axis parabolic mirror without any correction for the collection efficiency. (**b**) Emission spectra in a CW as a function of the sample holder temperature, for a set of currents starting at the maximum current of 580 mA and decreasing in 20 mA steps. The linewidth is limited by the resolution of the FTIR spectrometer.

The variation of the threshold current density with the temperature is presented in Figure 4b. The exponential increase of J_{th} was fitted with a characteristic temperature T0 = 180 K in pulsed mode for FP and DFB lasers. In a CW, T0 was 130 K for the Λ = 2.666 µm QCL presented in Figure 5 and 140 K for the Λ = 2.590 µm QCL presented in Figure 6. The comparison of the J_{th} values in pulsed and CW operation showed that the internal temperature in the active region of the lasers operating in a CW is 50–60 K higher relative to the temperature of the sample holder for the maximum current density of 1.4 kA/cm^2. This corresponds to thermal resistances of about 9 K/W, which is typical for the used epi-side down mounting technique and this geometry of QCL ridges. Similar results were obtained in a CW with an FP laser. These values are also consistent with the observed relative spectral shift of laser spectra between pulsed and CW operation. These results could be improved in future work by the use of a different passivation material and thick electroplated gold on the top contact.

4. Conclusions

In summary, we have fabricated and studied single frequency QCLs based on the InAs/AlSb material system emitting at a wavelength close to 17.7 µm, with CW output powers in the mW range. This is the longest wavelength recorded for DFB QCLs operating in a CW at room temperature. It should be noted that this wavelength is also the longest for CW operation of any QCLs and semiconductor lasers in general. These lasers can be operated in Peltier cooled systems, which can enable new spectroscopic applications in this almost unexplored spectral range from 11 to 18 µm.

Author Contributions: Investigation: H.N.V., Z.L., H.P., M.B., A.N.B., and R.T.; writing—original draft preparation: R.T.; writing—review and editing: Z.L., M.B., and A.N.B.; supervision: R.T. and A.N.B.

Funding: This research was partly funded by the French program on "Investments for the future" (Equipex EXTRA, project n° ANR-11-EQPX-0016).

Conflicts of Interest: The authors declare no conflict of interest.

References

1. Vitiello, M.S.; Scalari, G.; Williams, B.; Natale, P.D. Quantum cascade lasers: 20 years of challenges. *Opt. Express* **2015**, *23*, 5167–5182. [CrossRef] [PubMed]
2. Laffaille, P.; Moreno, J.C.; Teissier, R.; Bahriz, M.; Baranov, A.N. High temperature operation of short wavelength InAs-based quantum cascade lasers. *AIP Adv.* **2012**, *2*, 022119. [CrossRef]

3. Bahriz, M.; Lollia, G.; Baranov, A.N.; Teissier, R. High temperature operation of far infrared (lambda approximate to 20 μm) InAs/AlSb quantum cascade lasers with dielectric waveguide. *Opt. Express* **2015**, *23*, 1523–1528. [CrossRef] [PubMed]
4. Cathabard, O.; Teissier, R.; Devenson, J.; Moreno, J.C.; Baranov, A.N. Quantum cascade lasers emitting near 2.6 μm. *Appl. Phys. Lett.* **2010**, *96*, 141110. [CrossRef]
5. Walther, C.; Scalari, G.; Faist, J.; Beere, H.; Ritchie, D. Low frequency terahertz quantum cascade laser operating from 1.6 to 1.8 THz. *Appl. Phys. Lett.* **2006**, *89*, 231121. [CrossRef]
6. Faist, J.; Gmachl, C.; Capasso, F.; Sirtori, C.; Sivco, D.L.; Baillargeon, J.N.; Cho, A.Y. Distributed feedback quantum cascade lasers (vol 70, pg 2670, 1997). *Appl. Phys. Lett.* **1997**, *71*, 986. [CrossRef]
7. Xie, F.; Caneau, C.; LeBlanc, H.P.; Coleman, S.; Hughes, L.C.; Zah, C. Continuous wave operation of distributed feedback quantum cascade lasers with low threshold voltage and low power consumption. In *Novel in-Plane Semiconductor Lasers Xi*; Belyanin, A.A., Smowton, P.M., Eds.; Spie-Int Soc Optical Engineering: Bellingham, WA, USA, 2012; Volume 8277, p. 82770S. ISBN 978-0-8194-8920-3.
8. Lu, Q.Y.; Bai, Y.; Bandyopadhyay, N.; Slivken, S.; Razeghi, M. Room-temperature continuous wave operation of distributed feedback quantum cascade lasers with watt-level power output. *Appl. Phys. Lett.* **2010**, *97*, 231119. [CrossRef]
9. Xie, F.; Caneau, C.; LeBlanc, H.P.; Coleman, S.; Ho, M.-T.; Hughes, L.C.; Zah, C. Room temperature continuous wave operation of long Wavelength (9–11 μm) distributed feedback quantum cascade lasers for glucose detection. In *Novel in-Plane Semiconductor Lasers Xii*; Belyanin, A.A., Smowton, P.M., Eds.; Spie-Int Soc Optical Engineering: Bellingham, WA, USA, 2013; Volume 8640, p. 864016. ISBN 978-0-8194-9409-2.
10. Saeedi, K.; Szech, M.; Dluhy, P.; Salvail, J.Z.; Morse, K.J.; Riemann, H.; Abrosimov, N.V.; Nötzel, N.; Litvinenko, K.L.; Murdin, B.N.; et al. Optical pumping and readout of bismuth hyperfine states in silicon for atomic clock applications. *Sci. Rep.* **2015**, *5*, 10493. [CrossRef]
11. Kajita, M. Precise Measurement of Transition Frequencies of Optically Trapped 40Ca19F Molecules. *J. Phys. Soc. Jpn.* **2018**, *87*, 104301. [CrossRef]
12. Tokunaga, S.K.; Hendricks, R.J.; Tarbutt, M.R.; Darquié, B. High-resolution mid-infrared spectroscopy of buffer-gas-cooled methyltrioxorhenium molecules. *New J. Phys.* **2017**, *19*, 053006. [CrossRef]
13. Tredicucci, A.; Gmachl, C.; Capasso, F.; Sivco, D.L.; Hutchinson, A.L.; Cho, A.Y. Long wavelength superlattice quantum cascade lasers at lambda similar or equal to 17 μm. *Appl. Phys. Lett.* **1999**, *74*, 638–640. [CrossRef]
14. Huang, X.; Charles, W.O.; Gmachl, C. Temperature-insensitive long-wavelength (lambda approximate to 14 μm) Quantum Cascade lasers with low threshold. *Opt. Express* **2011**, *19*, 8297–8302. [CrossRef] [PubMed]
15. Fujita, K.; Yamanishi, M.; Edamura, T.; Sugiyama, A.; Furuta, S. Extremely high T0-values (~450 K) of long-wavelength (~15 μm), low-threshold-current-density quantum-cascade lasers based on the indirect pump scheme. *Appl. Phys. Lett.* **2010**, *97*, 201109. [CrossRef]
16. Ohtani, K.; Beck, M.; Süess, M.J.; Faist, J.; Andrews, A.M.; Zederbauer, T.; Detz, H.; Schrenk, W.; Strasser, G. Far-Infrared Quantum Cascade Lasers Operating in the AlAs Phonon Reststrahlen Band. *ACS Photonics* **2016**, *3*, 2280–2284. [CrossRef]
17. Rochat, M.; Hofstetter, D.; Beck, M.; Faist, J. Long-wavelength (lambda approximate to 16 μm), room-temperature, single-frequency quantum-cascade lasers based on a bound-to-continuum transition. *Appl. Phys. Lett.* **2001**, *79*, 4271–4273. [CrossRef]
18. Fuchs, P.; Semmel, J.; Friedl, J.; Hoefling, S.; Koeth, J.; Worschech, L.; Forchel, A. Distributed feedback quantum cascade lasers at 13.8 μm on indium phosphide. *Appl. Phys. Lett.* **2011**, *98*, 211118. [CrossRef]
19. Loghmari, Z.; Bahriz, M.; Thomas, D.D.; Meguekam, A.; Van, H.N.; Teissier, R.; Baranov, A.N. Room temperature continuous wave operation of InAs/AlSb-based quantum cascade laser at approximate to 11 μm. *Electron. Lett.* **2018**, *54*, 1045–1046. [CrossRef]
20. Baranov, A.N.; Bahriz, M.; Teissier, R. Room temperature continuous wave operation of InAs-based quantum cascade lasers at 15 μm. *Opt. Express* **2016**, *24*, 18799–18806. [CrossRef] [PubMed]
21. Loghmari, Z.; Bahriz, M.; Meguekam, A.; Teissier, R.; Baranov, A.N. InAs-based quantum cascade lasers emitting close to 25 μm. *Electron. Lett.* **2019**, *55*, 144–145. [CrossRef]
22. Yu, J.S.; Slivken, S.; Darvish, S.R.; Evans, A.; Gokden, B.; Razeghi, M. High-power, room-temperature, and continuous-wave operation of distributed-feedback quantum-cascade lasers at lambda similar to 4.8 μm. *Appl. Phys. Lett.* **2005**, *87*, 041104. [CrossRef]

23. Orfanos, I.; Sphicopoulos, T.; Tsigopoulos, A.; Caroubalos, C. A Tractable Above-Threshold Model for the Design of Dfb and Phase-Shifted Dfb Lasers. *IEEE J. Quantum Electron.* **1991**, *27*, 946–956. [CrossRef]
24. Slivken, S.; Bandyopadhyay, N.; Tsao, S.; Nida, S.; Bai, Y.; Lu, Q.Y.; Razeghi, M. Sampled grating, distributed feedback quantum cascade lasers with broad tunability and continuous operation at room temperature. *Appl. Phys. Lett.* **2012**, *100*, 261112. [CrossRef]
25. Wang, D.-B.; Zhang, J.-C.; Cheng, F.-M.; Zhao, Y.; Zhuo, N.; Zhai, S.-Q.; Wang, L.-J.; Liu, J.-Q.; Liu, S.-M.; Liu, F.-Q.; et al. Stable Single-Mode Operation of Distributed Feedback Quantum Cascade Laser by Optimized Reflectivity Facet Coatings. *Nanoscale Res. Lett.* **2018**, *13*, 37. [CrossRef] [PubMed]
26. Carras, M.; Garcia, M.; Marcadet, X.; Parillaud, O.; De Rossi, A.; Bansropun, S. Top grating index-coupled distributed feedback quantum cascade lasers. *Appl. Phys. Lett.* **2008**, *93*, 011109. [CrossRef]
27. Chastanet, D.; Bousseksou, A.; Lollia, G.; Bahriz, M.; Julien, F.H.; Baranov, A.N.; Teissier, R.; Colombelli, R. High temperature, single mode, long infrared (lambda = 17.8 μm) InAs-based quantum cascade lasers. *Appl. Phys. Lett.* **2014**, *105*, 111118. [CrossRef]